Steel and Composite Structures, *Vol. 36, No. 6 (2020) 643-656*
DOI: https://doi.org/10.12989/scs.2020.36.6.643

Static analysis of multilayer nonlocal strain gradient nanobeam reinforced by carbon nanotubes

Ahmed Amine Daikh*[1,2], Ahmed Drai[3,4], Mohamed Sid Ahmed Houari[1] and Mohamed A. Eltaher[5,6]

[1]Department of Civil Engineering, Laboratoire d'Etude des Structures et de Méecanique des Matéeriaux, Mascara, Algeria
[2]Mechanics of Structures and Solids Laboratory, Faculty of Technology, University of Sidi Bel Abbes, Sidi Bel Abbes, Algeria
[3]Department of Mechanical Engineering, Mustapha STAMBOULI, University of Mascara, 29000, Algeria
[4]LABAB Laboratory of ENPO, Oran, 31000, Algeria
[5]Faculty of Engineering, Department of Mechanical Engineering, King Abdulaziz University, P.O. Box 80204, Jeddah, Saudi Arabia
[6]Faculty of Engineering, Department of Mechanical Design and Production, Zagazig University, P.O. Box 44519, Zagazig, Egypt

(*Received July 5, 2020, Revised August 21, 2020, Accepted August 28, 2020*)

Abstract. This article presents a comprehensive static analysis of simply supported cross-ply carbon nanotubes reinforced composite (CNTRC) laminated nanobeams under various loading profiles. The nonlocal strain gradient constitutive relation is exploited to present the size-dependence of nano-scale. New higher shear deformation beam theory with hyperbolic function is proposed to satisfy the zero-shear effect at boundaries and parabolic variation through the thickness. Carbon nanotubes (CNTs), as the reinforced elements, are distributed through the beam thickness with different distribution functions, which are, uniform distribution (UD-CNTRC), V- distribution (FG-V CNTRC), O- distribution (FG-O CNTRC) and X- distribution (FG-X CNTRC). The equilibrium equations are derived, and Fourier series function are used to solve the obtained differential equation and get the response of nanobeam under uniform, linear or sinusoidal mechanical loadings. Numerical results are obtained to present influences of CNTs reinforcement patterns, composite laminate structure, nonlocal parameter, length scale parameter, geometric parameters on center deflection ad stresses of CNTRC laminated nanobeams. The proposed model is effective in analysis and design of composite structure ranging from macro-scale to nano-scale.

Keywords: static and stress analysis; Nonlocal strain gradient theory; hyperbolic shear deformation theory; carbon nanotubes reinforced nanobeams; fourier series

1. Introduction

The multilayered composites are widely used in various engineering structures such us aircraft, submarines, space-station structures etc., due to their high stiffness and strength to weight ratios caused by fiber reinforcement. Recently, to improve mechanical, electrical, and thermal properties of composite structures, carbon nanotubes (CNTs) are proposed and used instead of the conventional fibers due to their excellent properties. In other hand, in the literature, a considerable research works is performed on the mechanical response of the structures with functionally graded material properties such as functionally graded (FG) carbon nanotube-reinforced composites (CNTRC), FG graphene-reinforced composites (GRC) and FG porous structure, functionally graded materials (FGMs).

FGMs are inhomogeneous composites with a smooth change in constituents and hence, their mechanical and physical properties along one or more directions. The use of this structures can effectively alleviate or eliminate the interfacial failure due to interlaminar shear stress and singularity of stresses at edges of the inner layers. Due to ideal properties of ceramics in heat conditions combined with the toughness of metals, the combination of ceramics and metals can lead to excellent materials. With the wide application of FGM structures, the researchers have been focused on the mechanical behaviors of FGMs. Some researchers have analyzed FG beams using the elasticity solutions (Sankar 2001, Zhong and Yu 2007, Ding *et al*. 2007, Lu *et al*. 2008, Ying *et al* 2008 and Hassaine and Daouadji 2013) which are analytically very difficult.

In other hand, some analytical solutions are performed based on the first order shear deformation theory FSDT Bouremana *et al*. 2013, Hadji *et al*. 2016, Almitani *et al.* 2020 and Eltaher *et al.* 2020). Due to the limitations of CBT and FSDT for the analysis of thick beams, higher order shear deformation theories HSDTs are developed by considering the transverse shear deformation. In the literature, various beam HSDT models have been proposed base on polynomial function (Kadoli *et al*. 2008, Hadji *et al*. 2015, Hadji *et al*. 2016, Avhad and Sayyad 2020), trigonometric function (Benatta *et al*. 2008), hyperbolic function (Ould Larbi *et al*. 2013, Zidi *et al*. 2017, Zouatnia *et al.* 2017, Sayyad and Ghugal 2018, Malikan and Eremeyev 2020) and exponential function (Aydogdu and Taskin 2007, Sallai *et al*. 2015, Hadji *et al*. 2015b). Also, the effect of thickness stretching is considered by Meradjah *et al.* (2015), Bourada *et al*. (2015), and Bouafia *et al*. (2016).

∗Corresponding author, Ph.D.
E-mail: daikh.ahmed.amine@gmail.com

http://www.techno-press.org/?journal=scs&subpage=8 ISSN: 1229-9367 (Print), 1598-6233 (Online)

The application of nonlocal theory in the mechanical response of nanobeams is quite extensive (Eltaher *et al.* 2013, Chaht *et al*. 2015, Ahouel *et al.* 2016, Ebrahimi and Barati 2016a,b,c, Barati 2017, Ebrahimi and Barati 2017a,b,c, Barati *et al*. 2018, Bensaid *et al.* 2020, Mirjavadi et al. 2020). From the above-mentioned studies, it is found that nonlocal effect has a significant influence on the mechanical response of nanobeams. It is reported that the nonlocal elastic theory is extensively utilized to capture the size-dependent influence and can only provide stiffness softening effect on nanobeams.

Since complex fabrication processes of the FGMs, micro voids and porosities often occur. For this, the impact of porosity-dependent material properties on behavior of FG beams is investigated in various papers (Ait Atmane *et al*. 2017, Akbaş 2017, Fouda *et al.* 2017, Eltaher *et al*. 2018, Zouatnia *et al.* 2019, Hadji *et al*. 2019, Zghal *et al.* 2020, Salari *et al*. 2020, Zhao *et al*. 2020, Tran *et al.* 2020, Hamed *et al*. 2020). In addition to the FGMs, and due to their wide applications in separation, combustion synthesis, and lightweight structural materials, porous materials beams have been investigated by many researches (Fahsi *et al.* 2013, Chen *et al*. 2015 and Heshmati and Daneshmand 2018) to solve some engineering problems.

Due to their low density, tensile strength and high elastic modulus, carbon nanotubes (CNTs) were considered as an excellent candidate for the reinforcement of polymer composites (Salvetat Rubio 2002). After the invention of these structures, various research papers are performed to evaluate the mechanical problems of the CNTs reinforced composite (CNTRC) beams. For example, Yas and Samadi (2012) investigated the mechanical response of single-walled CNTRC beams supported on elastic foundations by employing Timoshenko beams theory (TBT) and differential quadrature method (DQM). Wattanasakulpong and Ungbhakorn (2013) analyzed buckling, vibration and bending behavior of CNTRC beams with various patterns reinforcement using an analytical solution. The impact of thermal loadings on mechanical response of CNTRC beams is carried out by Mayandi and Jeyaraj (2013). Finite element element, nonlocal elasticity and the TBT are used by Pradhan and Mandal (2013) to analyze the behavior of CNTRC beam including thermal effect. Ghorbanpour Arani and Zamani (2018) investigated the effect of modified Vlasov model foundation on bending of agglomerated CNTRC beams based on the classical beam theory (CBT) and the iterative technique. By considering small scale effect, Borjalilou *et al.* (2019) proposed closed-form solutions for static of cantilever, simply supported and clamped CNTRC nanobeams. In addition to CNTs, in order to produce high-performance composite structures, graphene platelets (GPLs) is proposed as reinforcement and their mechanic behavior is studied in some researches (Shen *et al.* 2017, Feng *et al.* 2017, Sahmani *et al.* 2018, Wang *et al.* 2019, Anirudh *et al.* 2020, Sobhy 2020). Daikh *et al.* (2020) investigated static bending of multilayered carbon nanotube-reinforced composite plates using various shear deformation plate theories.

In the current work, the influence of size-dependent on static deflection and stresses of SWCNTs reinforced multilayered composite nanobeam is presented by employing a novel hyperbolic shear deformation theory and nonlocal strain gradient elasticity, for the first time. The equilibrium equations are derived and solved by using Navier procedure for nanobeams with simply supported boundary conditions. The rest of the manuscript is organized as follows: - section 2 illustrates the modeling of CNTRC laminated beams and its constitutive equations. The equilibrium equation for classical laminated FG-CNTs laminated beam by using new hyperbolic shear deformation theory is presented in section 3. Through section 4, equilibrium equation for nonlocal strain gradient FG-CNTs nanobeam is derived in details. Exact solution by Navier procedure for nanobeams is presented in section 5. Loads types and numerical results are presented in sections 6 and 7, respectively. Main points and outcomes are summarized in conclusion section.

2. Modeling of CNTRC laminated beams

As shown in Fig. 1, uniform CNTRC laminated beam of length *L*, and thickness *h* is considered. Each lamina of the beam is reinforced by SWCNTs according to different distributions of gradation function as presented in Fig. 1(b). The selected CNTs distribution schemes are mathematically expressed by the volume fraction of CNTs V_{cnt} as follows, Daikh *et al*. (2020):

UD CNTRC laminated beam

$$V_{cnt} = V_{cnt}^{*} \tag{1}$$

FG-V CNTRC laminated beam

$$V_{cnt} = 1 - \left(\frac{2z - z_{(k)} - z_{(k-1)}}{z_{(k)} - z_{(k-1)}}\right) V_{cnt}^{*} \tag{2}$$

FG-O CNTRC laminated beam

$$V_{cnt} = 2\left(1 - \frac{\left|2|z| - |z_{(k-1)} + z_{(k)}|\right|}{z_{(k)} - z_{(k-1)}}\right) V_{cnt}^{*} \tag{3}$$

FG-X CNTRC laminated beam

$$V_{cnt} = 2\,\frac{\left|2|z| - |z_{(k-1)} + z_{(k)}|\right|}{z_{(k)} - z_{(k-1)}} V_{cnt}^{*} \tag{4}$$

where UD CNTRC indicate the uniform distribution, and FG-V CNTRC, FG-O CNTRC and FG-X CNTRC indicate the non-uniform functionally graded distributions. $z_{(k)}$ and $z_{(k-1)}$ are the vertical positions of the bottom surface and the top surface of the k^{th} layer of the laminated beam. V_{cnt}^{*} denote the given volume fraction of CNTs, and can be expressed as

$$V_{cnt}^{*} = \frac{W_{cnt}}{W_{cnt} + (\rho_{cnt}/\rho_m)(1 - W_{cnt})} \tag{5}$$

where W_{cnt}, ρ_{cnt} and ρ_m are the CNTs mass fraction, CNTs mass density and polymer matrix mass density, respectively.

The effective Young's modulus (*E*) and shear modulus (*G*) of a CNTRC sheet are given as

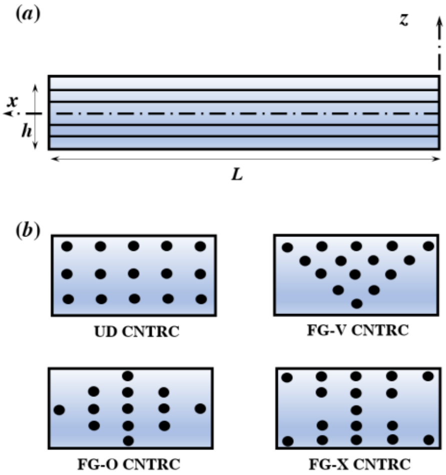

Fig. 1 Geometry and cross-sections of FG-CNTRC Laminated beam

$$E_{11}^k = \eta_1 V_{cnt}^k E_{11}^{cnt} + V_p^k E_p$$
$$\frac{\eta_2}{E_{22}^k} = \frac{V_{cnt}^k}{E_{22}^{cnt}} + \frac{V_p^k}{E_p} \tag{6}$$
$$\frac{\eta_3}{G_{12}^k} = \frac{V_{cnt}^k}{G_{12}^{cnt}} + \frac{V_p^k}{G_p}$$

Poisson's ratio $\nu_{12}^k$and density ρ^k of each sheet can be expressed as

$$\nu_{12}^k = V_{cnt}^k \nu_{12}^{cnt} + V_p^k \nu_p \tag{7}$$

$$\rho^k = V_{cnt}^k \rho_{cnt} + V_p^k \rho_p \tag{8}$$

where E_{11}^k and E_{22}^k are the Young's modulus across the plane directions (x, z), and G_{12}^k is the shear modulus of the plate composites. The superscripts p and cnt refer to the properties of the polymer and the SWCNTs, respectively.

The CNT efficiency parameters η_i $(i = 1,2,3)$ are given by Wattanasakulpong and Ungbhakorn (2013):

For $V_{cnt}^* = 0.12$; $\eta_1 = 1.2833$, $\eta_2 = \eta_3 = 1.0556$.

For $V_{cnt}^* = 0.17$; $\eta_1 = 1.3414$,$\eta_2 = \eta_3 = 1.7101$.

For $V_{cnt}^* = 0.28$; $\eta_1 = 1.3238$,$\eta_2 = \eta_3 = 1.7380$.

3. Equilibrium equations for hyperbolic beam

Consider a rectangular CNTRC laminated plate composed of k^{th} layers, as shown in Fig 1. The displacement field of CNTRC laminated nanobeam based on HSDT can be expressed by

$$u(x, y, z) = u_0 - z\frac{\partial w_0}{\partial x} + f(z)\varphi_x$$
$$w(x, y, z) = w_0 \tag{9}$$

where u_0, v_0, and w_0, are the displacement components along the directions x, y and z. φ_1 and φ_2 are the rotations of the transverse normal around the axes x and y.

In the present study, the shear deformation along the thickness direction can be expressed by a hyperbolic function in the form

$$f(z) = \frac{h\left(\pi \cosh\left(\frac{\pi}{2}\right)\tanh\left(\frac{z}{h}\right) - \sinh\left(\frac{\pi z}{h}\right)\left(1 - \tanh\left(\frac{1}{2}\right)^2\right)\right)}{\pi\left(\tanh\left(\frac{1}{2}\right)^2 + \cosh\left(\frac{\pi}{2}\right) - 1\right)} \tag{10}$$

The kinematic strain components associated with the displacements are stated as

$$\varepsilon_{xx} = \varepsilon_{xx}^0 - z\varepsilon_{xx}^1 + f(z)\varepsilon_{xx}^2$$
$$\gamma_{xz} = \frac{df(z)}{dz}\varphi_x \tag{11}$$

in which

$$\varepsilon_{xx}^0 = \frac{\partial u}{\partial x}$$
$$\varepsilon_{xx}^1 = \frac{\partial^2 w}{\partial x^2} \tag{12}$$
$$\varepsilon_{xx}^2 = \frac{\partial \varphi_x}{\partial x}$$

The constitutive stress–strain relations for each layer (k) can be expressed as

$$\begin{Bmatrix} \sigma_{xx} \\ \sigma_{xz} \end{Bmatrix}^{(k)} = \begin{bmatrix} \bar{Q}_{11}^k & 0 \\ 0 & \bar{Q}_{55}^k \end{bmatrix} \begin{Bmatrix} \varepsilon_{xx} \\ \gamma_{xz} \end{Bmatrix}^{(k)} \tag{13}$$

where

$$\bar{Q}_{11}^k = Q_{11}cos^4\theta_k + 2(Q_{12} + 2Q_{66})sin^2\theta_k cos^2\theta_k + Q_{22}sin^4\theta_k$$
$$\bar{Q}_{55}^k = Q_{55}cos^2\theta_k + Q_{44}sin^2\theta_k \tag{14}$$

$$Q_{11} = \frac{E_{11}}{1 - \nu_{12}\nu_{21}}, Q_{22} = \frac{E_{22}}{1 - \nu_{12}\nu_{21}}, \quad Q_{12} = \frac{\nu_{12}E_{22}}{1 - \nu_{12}\nu_{21}},$$
$$Q_{44} = G_{23}, Q_{55} = G_{13}, Q_{66} = G_{12} \tag{15}$$

Here, Q_{ij} is the equvelent stiffness, $\bar{Q}_{ij}$ is the transormed stiffnes, θ_k denote the lamination angle of the k^{th} layer.

The principle of virtual work when applied to the beam leads to

$$\int_0^L \left[N_{xx}\frac{d\delta u}{\partial x} - M_{xx}\frac{d^2\delta w}{\partial x^2} + P_{xx}\frac{d\delta\varphi_x}{\partial x} + Q_{xz}\delta\varphi_x\right]\mathrm{d}x\mathrm{d}z - \int_0^L q(x)\mathrm{d}x = 0 \tag{16}$$

The stress resultants of the CNTRC nanoplate are related with the strains as the following forms

$$\begin{Bmatrix} N_{xx} \\ M_{xx} \\ P_{xx} \end{Bmatrix} = \sum_{k=1}^{n}\int_{h_{k-1}}^{h_k}\begin{Bmatrix} 1 \\ z \\ f(z) \end{Bmatrix}\sigma_{xx}{}^{(k)}\mathrm{d}z$$
$$Q_{xz} = \sum_{k=1}^{n}\int_{h_{k-1}}^{h_k}\frac{df(z)}{dz}\sigma_{xz}{}^{(k)}\mathrm{d}z \tag{17}$$

The force and moment resultants of the composite beam can be related to the total strains by

$$\begin{Bmatrix} N_{xx} \\ M_{xx} \\ P_{xx} \end{Bmatrix} = \begin{bmatrix} A_{11} & B_{11} & C_{11} \\ B_{11} & D_{11} & F_{11} \\ C_{11} & F_{11} & H_{11} \end{bmatrix}\begin{Bmatrix} \varepsilon_x^0 \\ \varepsilon_x^1 \\ \varepsilon_x^2 \end{Bmatrix}$$
$$Q_{xz} = A_{55}\gamma_{xz} \tag{18}$$

With

$$\{A_{11}, B_{11}, D_{11}, C_{11}, F_{11}, H_{11}\} = \sum_{k=1}^{n}\int_{h_{n-1}}^{h_n} Q_{11}{}^{(k)}\{1, z, z^2, f(z), zf(z), f(z)^2\}dz \tag{19}$$

$$A_{55} = \sum_{k=1}^{n}\int_{h_{k-1}}^{h_k} Q_{55}{}^{(k)}\left[\frac{df(z)}{dz}\right]^2 dz \tag{20}$$

The force and moment resultants can be defined in displacement fields as follows

$$N_{xx} = A_{11}\frac{\partial u_0}{\partial x} - B_{11}\frac{\partial^2 w_0}{\partial x^2} + C_{11}\frac{\partial\varphi_x}{\partial x}$$
$$M_{xx} = B_{11}\frac{\partial u_0}{\partial x} - D_{11}\frac{\partial^2 w_0}{\partial x^2} + F_{11}\frac{\partial\varphi_x}{\partial x}$$
$$P_{xx} = C_{11}\frac{\partial u_0}{\partial x} - F_{11}\frac{\partial^2 w_0}{\partial x^2} + H_{11}\frac{\partial\varphi_x}{\partial x}$$
$$Q_{xz} = A_{55}\varphi_x \tag{21}$$

Based on the virtual work principle, the equilibrium equations can be derived as

$$\frac{\partial N_{xx}}{\partial x} = 0$$
$$\frac{\partial^2 M_{xx}}{\partial x^2} - q = 0$$
$$\frac{\partial P_{xx}}{\partial x} - Q_{xz} = 0 \tag{22}$$

4. Nonlocal strain gradient theory laminated nanobeam

By the coupling physical impact of the strain gradient stress and nonlocal elastic stress fields, Lim *et al.* (2015) proposed a function of stresses as

$$\sigma_{ij} = \sigma_{ij}^{(0)} - \frac{d\sigma_{ij}^{(1)}}{dx} \tag{23}$$

where $\sigma_{ij}^{(0)}$ and $\sigma_{ij}^{(1)}$ are the classical stress corresponds to strain ε_{kl} and the higher-order stress $\sigma_{ij}^{(1)}$ corresponds to strain gradient $\varepsilon_{kl,x}$ respectively, and can be expressed as

$$\sigma_{ij}^{(0)} = \int_0^L C_{ijkl}\alpha_0(x, x', e_0a)\varepsilon_{kl,x}(x')dx'$$
$$\sigma_{ij}^{(1)} = l^2\int_0^L C_{ijkl}\alpha_1(x, x', e_1a)\varepsilon_{kl,x}(x')dx' \tag{24}$$

C_{ijkl} denote an elastic constant and l is the material length scale parameter introduced to consider the significance of the strain gradient stress field. e_0a and e_1a are the nonlocal parameters introduced to consider the significance of the nonlocal elastic stress field.

The nonlocal kernel functions $\alpha_0(x, x', e_0a)$ and $\alpha_1(x, x', e_1a)$ satisfy the developed conditions by Eringen (1983), The general constitutive relation become as

$$[1-(e_1a)^2\nabla^2][1-(e_0a)^2\nabla^2]\sigma_{ij} = C_{ijkl}[1-(e_1a)^2\nabla^2]\varepsilon_{kl} - C_{ijkl}l^2[1-(e_0a)^2\nabla^2]\nabla^2\varepsilon_{kl} \tag{25}$$

∇^2 is the Laplacian operator. In the present analysis, we assume the coefficient $e = e_0 = e_1$. The total nonlocal strain gradient constitutive relation can be stated as Ebrahimi and Barati (2018)

$$[1-\mu\nabla^2]\sigma_{ij} = C_{ijkl}[1-\lambda\nabla^2]\varepsilon_{kl} \tag{26}$$

where $\mu = (ea)^2$ and $\lambda = l^2$.

$$(1-(e_0a)^2\nabla^2)\sigma_{ij} = C_{ijkl}(1-l^2\nabla^2)\varepsilon_{kl} \tag{27}$$

Therefore, the constitutive relations for a nonlocal shear deformable CNTRC laminated nanobeam can be expressed as Daikh *et al.* (2019)

$$\sigma_{xx} - \mu\frac{\partial^2\sigma_{xx}}{\partial x^2} = \bar{Q}_{11}^k\left(\varepsilon_{xx} - \lambda\frac{\partial^2\varepsilon_{xx}}{\partial x^2}\right) \tag{28}$$

$$\sigma_{xz} - \mu\frac{\partial^2\sigma_{xx}}{\partial x^2} = \bar{Q}_{55}^k\left(\gamma_{xz} - \lambda\frac{\partial^2\gamma_{xz}}{\partial x^2}\right) \tag{29}$$

By inserting Eqs. (28) and (29) on the stress resultants relation in Eq (21), the following equations are obtained

$$N_{xx} - \mu\frac{\partial^2 N_{xx}}{\partial x^2} = \left(1-\lambda^2\frac{\partial^2}{\partial x^2}\right)\left[A_{11}\frac{\partial u_0}{\partial x} - B_{11}\frac{\partial^2 w_0}{\partial x^2} + C_{11}\frac{\partial\varphi_x}{\partial x}\right]$$
$$M_{xx} - \mu\frac{\partial^2 M_{xx}}{\partial x^2} = \left(1-\lambda^2\frac{\partial^2}{\partial x^2}\right)\left[B_{11}\frac{\partial u_0}{\partial x} - D_{11}\frac{\partial^2 w_0}{\partial x^2} + F_{11}\frac{\partial\varphi_x}{\partial x}\right]$$
$$P_{xx} - \mu\frac{\partial^2 P_{xx}}{\partial x^2} = \left(1-\lambda^2\frac{\partial^2}{\partial x^2}\right)\left[C_{11}\frac{\partial u_0}{\partial x} - F_{11}\frac{\partial^2 w_0}{\partial x^2} + H_{11}\frac{\partial\varphi_x}{\partial x}\right]$$
$$Q_{xz} - \mu\frac{\partial^2 Q_{xz}}{\partial x^2} = \left(1-\lambda\frac{\partial^2}{\partial x^2}\right)[A_{55}\varphi_x] \tag{30}$$

Based on the nonlocal strain gradient theory, the equilibrium equations for FG-CNTRC nanobeam can be written as

$$\left(1-\lambda\frac{\partial^2}{\partial x^2}\right)\left(A_{11}\frac{\partial^2 u_0}{\partial x^2} - B_{11}\frac{\partial^3 w_0}{\partial x^3} + C_{11}\frac{\partial^2\varphi_x}{\partial x^2}\right) = 0$$
$$\left(1-\lambda\frac{\partial^2}{\partial x^2}\right)\left(B_{11}\frac{\partial^3 u_0}{\partial x^3} - D_{11}\frac{\partial^4 w_0}{\partial x^4} + F_{11}\frac{\partial^3\varphi_x}{\partial x^3}\right) - \left(1-\mu\frac{\partial^2}{\partial x^2}\right)q = 0$$
$$\left(1-\lambda\frac{\partial^2}{\partial x^2}\right)\left(C_{11}\frac{\partial^2 u_0}{\partial x^2} - F_{11}\frac{\partial^3 w_0}{\partial x^3} + H_{11}\frac{\partial^2\varphi_x}{\partial x^2} - J_{66}\varphi_x^1\right) = 0 \tag{31}$$

5. Exact solutions for FG-CNTRC nanobeams

Functions of the displacements field that satisfy the simply-simply cross-ply laminated beams boundary conditions are developed as Fourier series as (Daikh 2020)

$$\begin{aligned} u_0 &= \sum_{m=1}^{\infty} U_m \cos(\beta x) \\ w_0 &= \sum_{m=1}^{\infty} W_m \sin(\beta x) \\ \varphi_x &= \sum_{m=1}^{\infty} X_m \cos(\beta x) \end{aligned} \tag{32}$$

where U_{mn}, V_{mn}, and X_{mn} are arbitrary parameters and $\beta = m\pi/L$. Substituting Eqs. (32) into Eqs. (31) give

$$\begin{bmatrix} -A_{11}(\beta^2+\lambda\beta^4) & B_{11}(\beta^3+\lambda\beta^5) & -C_{11}(\beta^2+\lambda\beta^4) \\ 0 & -D_{11}(\beta^4+\lambda\beta^6) & F_{11}(\beta^3+\lambda\beta^5) \\ symmetric & 0 & -H_{11}(\beta^2+\lambda\beta^4)-A_{55}(1+\lambda\beta^2) \end{bmatrix} \begin{Bmatrix} U_m \\ W_m \\ X_m \end{Bmatrix} = \begin{Bmatrix} 0 \\ (1+\mu\beta^2)Qm \\ 0 \end{Bmatrix} \tag{33}$$

6. Loads in consideration

To evaluate the results, the transverse loadings must be expressed using a Fourier expansion, which varies according to the type of load. three types of loads are considered (see Fig. 2):

6.1 Uniformly distributed load

In this case, the distributed uniform transverse applied load on the top surface of nanobeam, shown in Fig. 2(a), can be expressed as

$$q(x) = \sum_{m=1}^{\infty} Q_m \sin(\beta x) \tag{34}$$

where the coefficients of the Fourier expansion are given by

$$\begin{aligned} Q_m &= \frac{4q_0}{m\pi} \quad \text{for } m = 1,3,5,\dots \\ Q_m &= 0 \quad \text{for } m = 2,4,6,\dots \end{aligned} \tag{35}$$

6.2 Sinusoidal load

A composite laminated beam under a sinusoidal static load on the top surface $z = h/2$ acting in the transverse direction is considered, as shown in Fig. 2(b). The load form can be written as

$$q(x) = \sum_{m=1}^{\infty} q_0 \sin(\beta x) \tag{36}$$

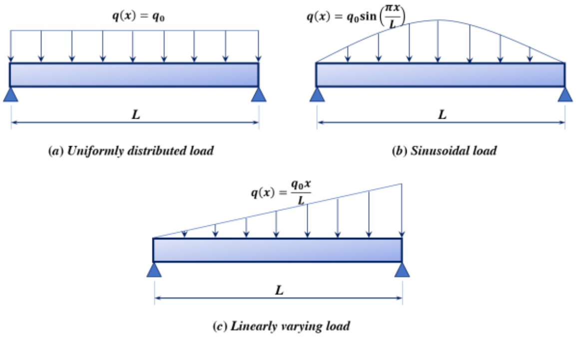

Fig. 2 Types of loads applied in the beam formulation

6.3 Linearly varying load

As illustrated in Fig. 2©, the linearly varying loads given by $q(x) = \frac{q_0 x}{L}$ acting on the surface $z = h/2$

$$\begin{aligned} Q_m &= -\frac{2q_0}{m\pi}\cos(m\pi) \quad \text{for } m = 1,3,5,\dots \\ Q_m &= 0 \quad \text{for } m = 2,4,6,\dots \end{aligned} \tag{37}$$

7. Numerical results

In this research, numerical results are presented to illustrate the stresses and deflections of CNTRC beams using a new hyperbolic higher order shear deformation beam theory. The boundary conditions considered are simply supported. The material chosen in this study is Poly methyl methacrylate (PMMA) as matrix material and the armchair (10,10) SWCNTs as a reinforcement.

Material properties of the matrix are $\nu^p = 0.3$, $\rho^p = 1190$ Kg/m^3 and $E^p = 2.5$GPa, and for the reinforcement $\nu^{cnt} = 0.19$, $\rho^{cnt} = 1400$ Kg/m^3, $E_{11}^{cnt} = 600$GPa, $E_{22}^{cnt} = 10$GPa and $G_{12}^{cnt} = 17.2$GPa. Numerical results are presented in terms of non-dimensional deflection and stresses parameters as

$$\bar{w} = \frac{10^2 E_p h^2}{L^4 q_0} w\left(\frac{L}{2}\right) \tag{38}$$

$$\bar{\sigma}_{xx} = -\frac{h}{Lq_0}\sigma_{xx}\left(\frac{L}{2}, \frac{h}{2}\right) \tag{39}$$

$$\bar{\tau}_{xz} = \frac{h}{Lq_0}\tau_{xz}(0,0) \tag{40}$$

Due to the existence limitation of similar work results for multilayered CNTRC nanobeams, the validation processes of the present model for its efficiency and precision are divided into two stages: (1) comparison study to validate the accuracy of the proposed hyperbolic shape function model and (2) parametric study to investigate the effects of several parameters independently.

In Table 1, comparison study is performed to validate the accuracy of the proposed HSDT with the results obtained by Wattanasakulpong and Ungbhakorn (2013) using Reddy's theory (TSDT). It is noted from results, that the proposed theory agrees well and very close with the obtained results by TSDT.

Table 2 illustrate the effect of nonlocal and length scale parameters on the dimensionless center deflection of CNTRC laminated beam (0°/90°) for different reinforcement patterns and various applied loadings. As predicted from this table, by the static deflection for a specific graduation type is proportional with the nonlocal parameter by fixing all other parameters. However, the static deflection proportional inversely with the strain gradient length scale under the same other loading and grading and distribution conditions. By fixing the nonlocal and stain gradient length scale parameter, it is noted the, the FG-X distribution has the highest stiffness and smallest deflection rather than other distributions, and, the FG-O has

Table 1 Nondimensional deflection and stresses in single layer UD-CNTRC beam

V^*_{cnt}	L/h	$\bar{w}$		$\bar{\sigma}_{xx}$		$\bar{\tau}_{xz}$	
		TSDT[(a)]	Present	TSDT[(a)]	Present	TSDT[(a)]	Present
Uniform load							
0,12	**10**	0.704	0.704	8.399	8.379	0.701	0.695
	15	0.524	0.524	11.849	11.836	0.716	0.710
	20	0.461	0.461	15.448	15.439	0.725	0.718
0,17	**10**	0.449	0.449	8.268	8.252	0.725	0.698
	15	0.344	0.344	11.762	11.751	0.719	0.713
	20	0.307	0.307	15.384	15.376	0.726	0.720
0,28	**10**	0.325	0.325	8.562	8.539	0.697	0.691
	15	0.235	0.235	11.959	11.942	0.714	0.708
	20	0.203	0.203	15.530	15.519	0.723	0.716
Sinusoidal load							
0,12	**10**	0.562	0.562	6.970	6.950	0.472	0.468
	15	0.416	0.416	9.716	9.702	0.475	0.470
	20	0.365	0.365	12.608	12.597	0.476	0.471
0,17	**10**	0.358	0.358	6.842	6.825	0.473	0.468
	15	0.273	0.273	9.630	9.618	0.476	0.470
	20	0.243	0.243	12.543	12.534	0.476	0.471
0,28	**10**	0.260	0.260	7.130	7.106	0.472	0.467
	15	0.187	0.187	9.824	9.808	0.475	0.470
	20	0.161	0.161	12.689	12.676	0.476	0.471
Linear load [(*)]							
0,12	**10**	-	0.176	-	2.100	-	0.350
	15	-	0.131	-	2.963	-	0.359
	20	-	0.115	-	3.863	-	0.363
0,17	**10**	-	0.112	-	2.068	-	0.352
	15	-	0.086	-	2.941	-	0.360
	20	-	0.077	-	3.846	-	0.364
0,28	**10**	-	0.081	-	2.141	-	0.348
	15	-	0.059	-	2.990	-	0.357
	20	-	0.051	-	3.883	-	0.362

(a) Results obtained by Wattanasakulpong, N. and Ungbhakorn, V. (2013).
(*) $\bar{\tau}_{xz} = (h/Lq_0)\tau_{xz}(L,0)$

the softest stiffness and highest deflection with respect to the other distributions. The deflection of FG-CNTRC nanobeam is smaller in case of linear loading type rather than uniform and sinusoidal load. However, the deflection in case of uniform load is higher than the other two cases.

Dimensionless axial and shear stresses of CNTRC beam $(0°/90°/0°)$ influenced by thickness ratio and the CNTs reinforcement pattern is illustrated in Table 3. As seen, by increasing the slenderness ration of the beam, the normal stress increased dramatically relative to the increasing in shear stress. For example, in case of uniform load and UD

Table 2 Effect of nonlocal and length scale parameters on the dimensionless center deflection of CNTRC laminated beam $(0°/90°)(V_{cnt}^{*}=0.12, a/h=10)$

μ	λ	Uniform load				Sinusoidal load				Linear load			
		UD	**FG-X**	**FG-O**	**FG-V**	**UD**	**FG-X**	**FG-O**	**FG-V**	**UD**	**FG-X**	**FG-O**	**FG-V**
0	**0**	2.5095	1.9108	3.7756	2.8855	1.9826	1.5100	2.9821	2.2776	0.6268	0.4770	0.9435	0.7206
	0,5	2.3955	1.8244	3.6034	2.7540	1.8894	1.4390	2.8419	2.1705	0.5983	0.4554	0.9005	0.6877
	1	2.2902	1.7443	3.4446	2.6326	1.8045	1.3744	2.7142	2.0730	0.5720	0.4354	0.8608	0.6574
	1,5	2.1931	1.6705	3.2983	2.5209	1.7270	1.3153	2.5976	1.9839	0.5478	0.4170	0.8242	0.6295
	2	2.1036	1.6024	3.1636	2.4179	1.6558	1.2611	2.4905	1.9022	0.5254	0.4000	0.7906	0.6038
0,5	**0**	2.6278	2.0005	3.9544	3.0221	2.0805	1.5845	3.1293	2.3900	0.6563	0.4994	0.9882	0.7547
	0,5	2.5095	1.9108	3.7756	2.8855	1.9826	1.5100	2.9821	2.2776	0.6268	0.4770	0.9435	0.7206
	1	2.3998	1.8276	3.6101	2.7590	1.8936	1.4422	2.8482	2.1753	0.5994	0.4562	0.9022	0.6890
	1,5	2.2986	1.7506	3.4574	2.6424	1.8122	1.3802	2.7258	2.0818	0.5741	0.4370	0.8640	0.6599
	2	2.2051	1.6795	3.3166	2.5348	1.7375	1.3233	2.6134	1.9960	0.5508	0.4193	0.8288	0.6330
1	**0**	2.7461	2.0901	4.1333	3.1587	2.1783	1.6590	3.2765	2.5024	0.6859	0.5218	1.0329	0.7888
	0,5	2.6235	1.9973	3.9477	3.0170	2.0759	1.5810	3.1224	2.3847	0.6553	0.4986	0.9866	0.7534
	1	2.5095	1.9108	3.7756	2.8855	1.9826	1.5100	2.9821	2.2776	0.6268	0.4770	0.9435	0.7206
	1,5	2.4040	1.8307	3.6165	2.7639	1.8974	1.4451	2.8539	2.1797	0.6005	0.4570	0.9038	0.6902
	2	2.3066	1.7566	3.4696	2.6517	1.8192	1.3855	2.7363	2.0899	0.5761	0.4385	0.8671	0.6622
1,5	**0**	2.8643	2.1797	4.3121	3.2953	2.2762	1.7335	3.4236	2.6148	0.7154	0.5442	1.0776	0.8229
	0,5	2.7375	2.0838	4.1199	3.1485	2.1691	1.6520	3.2626	2.4919	0.6837	0.5202	1.0296	0.7863
	1	2.6192	1.9941	3.9411	3.0119	2.0717	1.5778	3.1161	2.3799	0.6542	0.4978	0.9849	0.7522
	1,5	2.5095	1.9108	3.7756	2.8855	1.9826	1.5100	2.9821	2.2776	0.6268	0.4770	0.9435	0.7206
	2	2.4080	1.8337	3.6226	2.7686	1.9009	1.4478	2.8592	2.1838	0.6015	0.4578	0.9053	0.6914
2	**0**	2.9826	2.2694	4.4909	3.4319	2.3740	1.8081	3.5708	2.7272	0.7450	0.5665	1.1223	0.8570
	0,5	2.8514	2.1702	4.2921	3.2800	2.2623	1.7230	3.4029	2.5990	0.7122	0.5418	1.0726	0.8191
	1	2.7288	2.0773	4.1066	3.1384	2.1607	1.6456	3.2500	2.4822	0.6816	0.5186	1.0263	0.7837
	1,5	2.6150	1.9909	3.9347	3.0070	2.0679	1.5749	3.1103	2.3755	0.6531	0.4970	0.9833	0.7509
	2	2.5095	1.9108	3.7756	2.8855	1.9826	1.5100	2.9821	2.2776	0.6268	0.4770	0.9435	0.7206

distribution, the normal stress increased from 5.55 to 15.975 as the slenderness ration increased from 5 to 15, however, the shear stress increased from 0.65 to 0.715 at the same conditions. The highest normal stress is observed in case of FG-X and smallest normal stress is noticed at FG-O, by fixing other conditions, such as loading and slenderness ratio. It is noticed that the shear stress is dependent implicitly on loading type, gradation type and slenderness ratio.

Fig. 3 shows the dimensionless deflection of single layer UD CNTRC beam along the mid-plane longitudinal direction x under sinusoidal, uniform and linear loadings using various volume fraction values. Because of the symmetric distribution of the applied loads, the maximum value of deflections occurs at a point on the center of beam for the uniform and the sinusoidal loads. it is noted that the dimensionless central deflection decreases with the increase in the CNT volume fraction, because the increase of the latter improves the flexural stiffness of the beam

The deflection response of CNTRC laminated beam $(0°/90°)$ subjected to sinusoidal loads for various CNTs reinforcement patterns is plotted in Fig. 4. It is worth to note that the FG-O CNTRC laminated beam has the maximum deflection, whereas, the minimum value is for the FG-X CNTRC beams.

The effect of CNTR laminated beam length-to-thickness ratio L/h on the center deflection is shown in Fig. 5. The increase of length-to-thickness ratio lead to decrement on deflections wherever the CNTs reinforcement pattern is. It is revealed that as the value of nonlocal parameter μ increases, the dimensionless center deflection decreases. therefore, it can be concluded that the inclusion of size effects leads to the reduction of the stiffness of the CNTRC laminated beams .On the other hand, the center deflection increases with decreasing of the length scale parameter λ.

Table 3 Nondimensional normal and shear stresses of CNTRC beam $(0°/90°/0°)$ $(V^*_{cnt} = \mathbf{0.12})$

Load type		$L/h = 5$		$L/h = 10$		$L/h = 20$	
		$\bar{\sigma}_{xx}$	$\bar{\tau}_{xz}$	$\bar{\sigma}_{xx}$	$\bar{\tau}_{xz}$	$\bar{\sigma}_{xx}$	$\bar{\tau}_{xz}$
Uniform load	**UD**	5.550	0.650	8.610	0.693	15.975	0.715
	FG-X	9.863	0.548	15.975	0.589	30.073	0.609
	FG-O	0.163	0.792	0.244	0.829	0.446	0.848
	FG-V	0.174	0.663	0.264	0.700	0.485	0.719
Sinusoidal load	**UD**	4.759	0.453	7.129	0.464	13.027	0.467
	FG-X	8.373	0.385	13.173	0.396	24.493	0.399
	FG-O	0.551	0.364	0.549	0.203	0.5417	0.142
	FG-V	0.150	0.458	0.219	0.467	0.396	0.469
Linear load (*)	**UD**	1.387	0.325	2.152	0.173	3.994	0.179
	FG-X	2.466	0.274	3.994	0.147	7.518	0.152
	FG-O	0.212	0.111	0.207	0.061	0.396	0.049
	FG-V	0.043	0.332	0.066	0.175	0.121	0.180

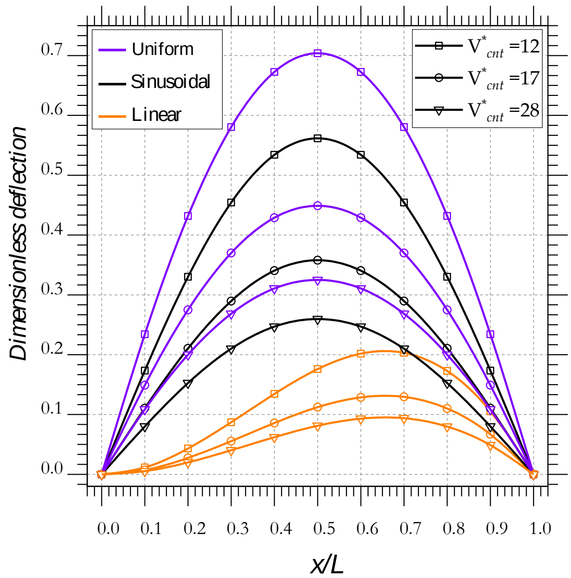

Fig. 3 Dimensionless deflection of single layer UD CNTRC beam under sinusoidal, uniform and linear loads

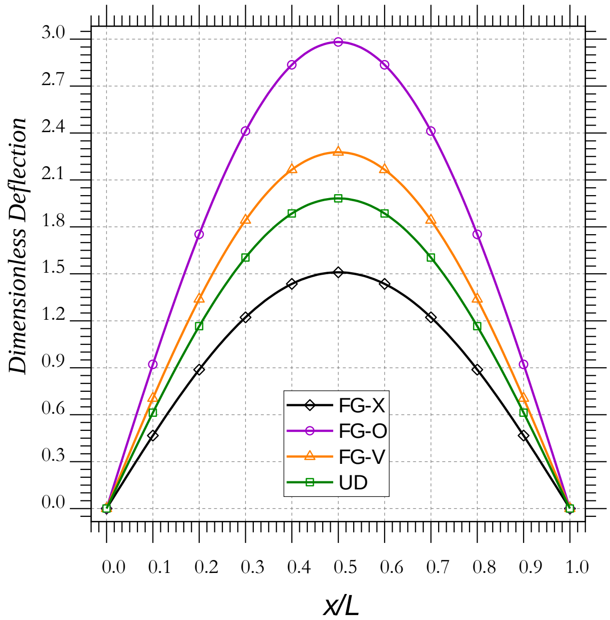

Fig. 4 Dimensionless deflection of various pattern of CNTRC laminated beam $(0°/90°)$ under sinusoidal load

The effect of number of layers on the deflection of CNTRC laminated beam $(0°/90°)_N$ is tabulated in Table 4, where the increase of number of layers lead to decrement of deflections due to the enhancement of stiffness of the beam structure. The stiffness enhancement is pronounced in by changing the number of layers from 1 to 2 and from 2 to 5. By increasing the number of layers more than 5 layers, the enhancement of stiffness becomes insignificant, as predicted from Table 4.

Effect of number of layers on dimensionless center deflection of UD and FG CNTRC laminated beams $(0°/90°)_N$ subjected to sinusoidal loading is plotted in Fig. 7. It is clear that, for various CNTs reinforcement patterns, the increase of number of layers lead to decrement of deflections. For $N \geq 4$, the results are almost constant regardless the CNTs reinforcement distribution.

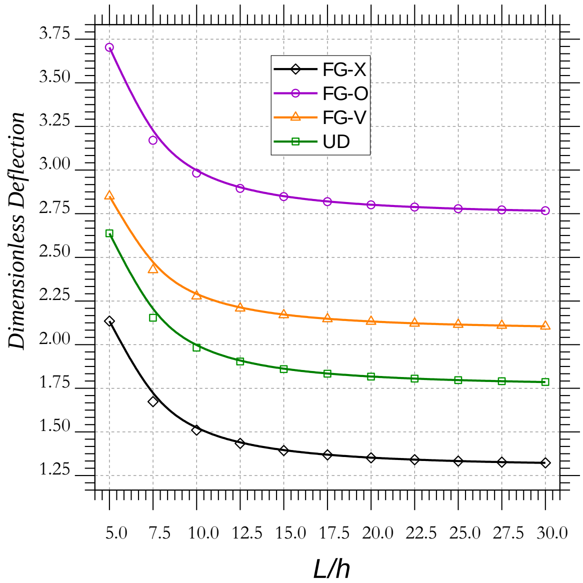

Fig. 5 Dimensionless deflection of various pattern of CNTRC laminated beam $(0°/90°)$ versus geometric parameter L/h

Table 4 Effect of number of layers on the dimensionless center deflection of CNTRC laminated beam $(0°/90°)_N$ $(a/h = 10)$

	N	UD	FG-X	FG-O	FG-V
0.12	**1**	1.9826	1.5100	2.9821	2.2776
	2	0.9749	0.9414	1.0110	0.9631
	5	0.8637	0.8592	0.8681	0.8608
	10	0.8498	0.8487	0.8508	0.8490
0.17	**1**	1.2884	0.9839	1.9111	1.4670
	2	0.6351	0.6127	0.6579	0.6284
	5	0.5620	0.5585	0.5643	0.5598
	10	0.5529	0.5516	0.5530	0.5519
0.28	**1**	0.4401	0.6743	1.3857	1.0707
	2	0.4401	0.4199	0.4517	0.4299
	5	0.3904	0.3836	0.3877	0.3842
	10	0.3841	0.3789	0.3799	0.3791

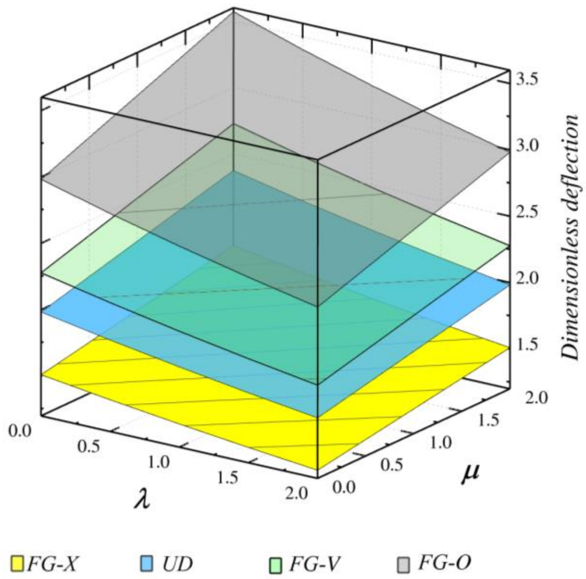

Fig. 6 Effect of nonlocal and length scale parameters on dimensionless center deflection of UD and FG CNTRC laminated beams $(0°/90°)$ $(a/h = 10)$

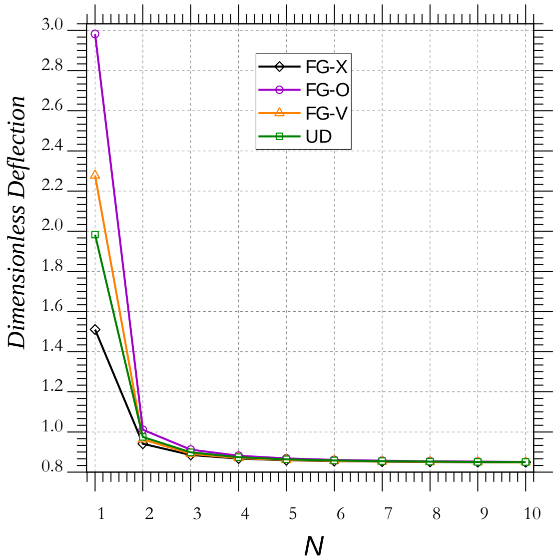

Fig. 7 Effect of number of layers on dimensionless deflection of UD and FG CNTRC laminated beams$(0°/90°)_N$

To clearly understand normal stresses $\bar{\sigma}_{xx}$ and shear stresses $\bar{\tau}_{xz}$ variations in CNTRC laminated beam $(0°/90°/0°)$, Figs. 8 and 9 show the plots of the results across the beam thickness with different CNT distribution patterns and by considering the effect of nonlocal and length to scale parameters. Dimensionless normal stresses $\bar{\sigma}_{xx}$ through the thickness of various CNTRC laminated beams are plotted.

For the FG-O CNTRC beam, having zeroth carbon nanotubes on the top and bottom layer surfaces, the normal stresses $\bar{\sigma}_{xx}$ are almost continuous at the laminate interfaces, whereas the stresses $\bar{\sigma}_{xx}$ for the other types are discontinuous. Moreover, the highest normal stresses through-the-thickness are at the point that have the maximum values of CNTs volume fraction. It can be observed that the CNTRC beam with the parameters $\mu = 2$ and $\lambda = 0$ yields the maximum tensile (compressive) stresses, whereas the minimum stresses are for $\mu = 0$ and $\lambda = 2$.

Fig. 9 illustrated the variation of dimensionless stresses $\bar{\tau}_{xz}$ across the CNTRC beam thickness. For the UD

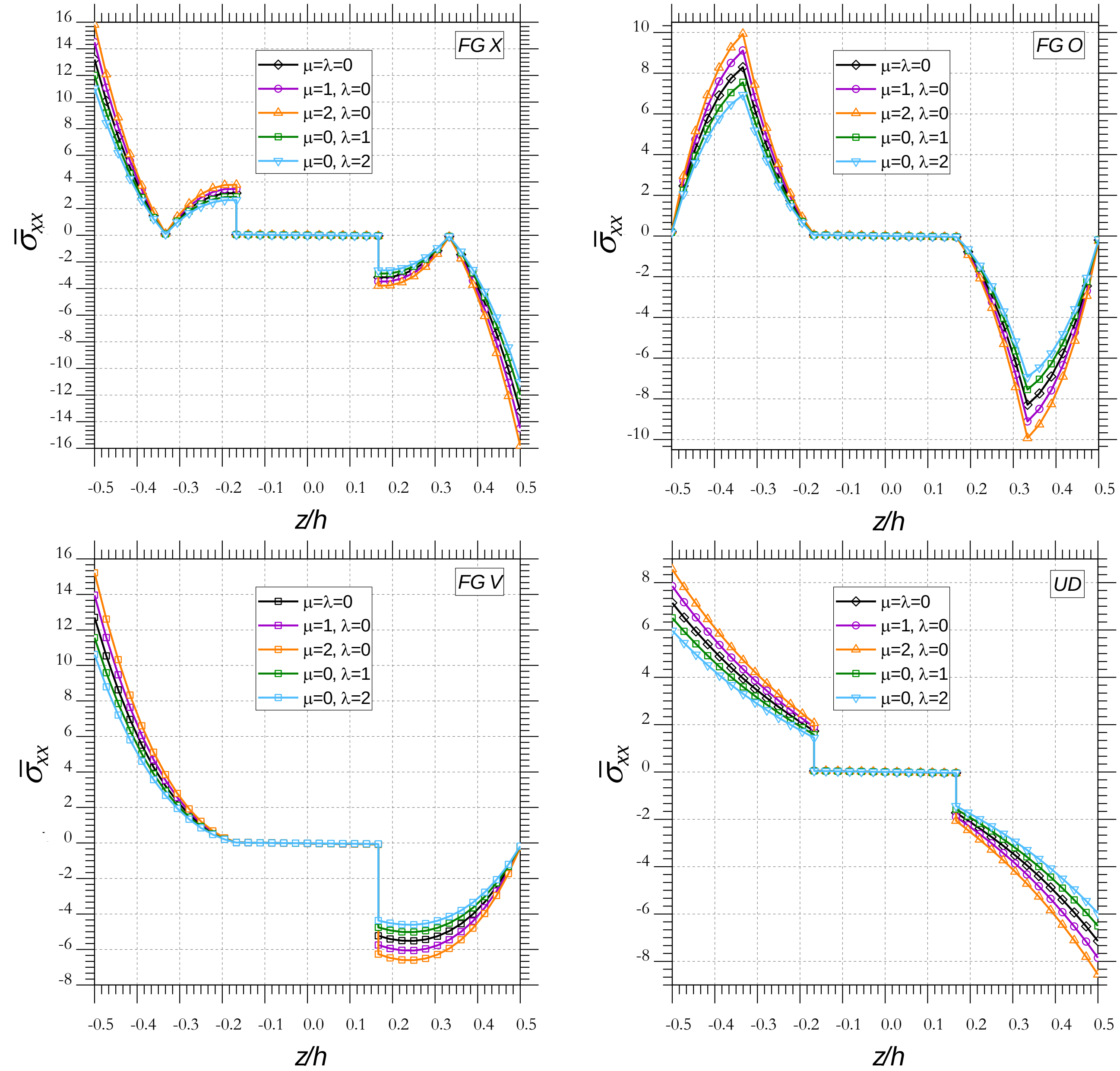

Fig. 8 Dimensionless stresses $\bar{\sigma}_{xx}$ of CNTRC laminated beam $(0°/90°/0°)$

CNTRC and FG-O CNTRC laminated beams, the maximum value of stresses $\bar{\tau}_{xz}$ occurs at a point on the mid-plane. The stresses $\bar{\tau}_{xz}$ has a continuous and smooth variation in the case of uniform CNTs distribution.

It can be observed that the maximum value occurs at a point on the mid-plane for the FG-O and UD CNTRC beams. For the FG-X CNTRC beams, maximum values occurs at the interfaces.

8. Conclusions

Size dependent bending behavior of CNTRC laminated nanobeams under various mechanical loadings is studied for the first time via the new hyperbolic shear deformation plate theory in conjunction with nonlocal strain gradient theory. Several numerical results are carried out to investigate transverse displacement and stresses of four types of reinforcement material distributions, a uniform distribution UD and three functionally graded (FG) distributions, through the beam thickness. An analytical solution is carried out to assess the influence of CNTs reinforcement patterns, composite laminate structure, nonlocal and length scale parameter, and geometric system on deflection and stresses of CNTRC laminated nanobeams. The numerical examples show that:

- ✓ The inclusion of size effects leads to the reduction of the stiffness of the CNTRC laminated nanobeams, where the increase of nonlocal parameter μ increases the dimensionless deflection. Unlike the nonlocality effect, the dimensionless deflections decrease by increasing of the length scale parameter λ.

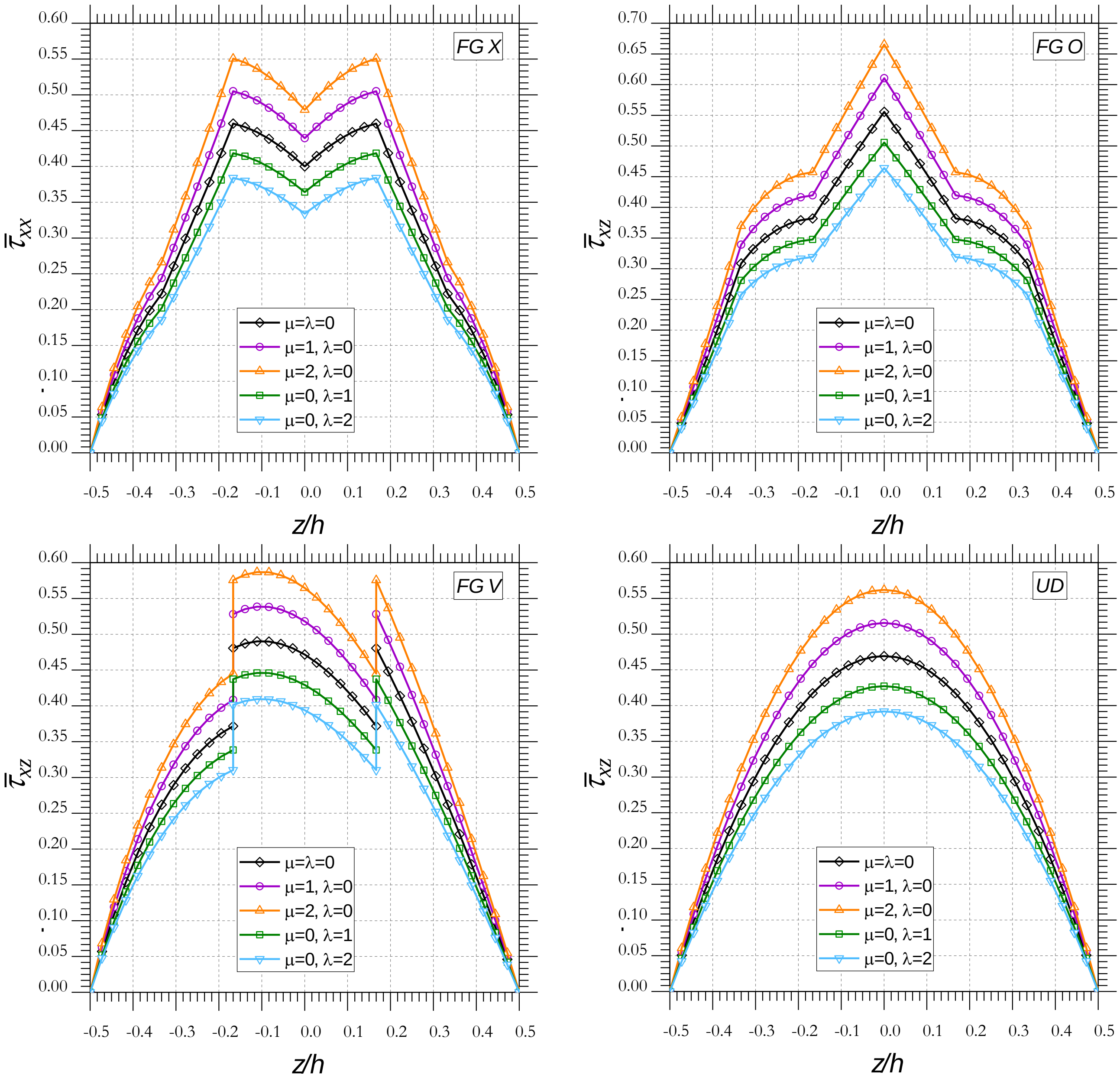

Fig. 9 Dimensionless stresses $\bar{\tau}_{xz}$ of CNTRC laminated beam $(0°/90°/0°)$

- ✓ The increase of number of layers lead to increment of the strength of the CNTRC laminated nanobeams, thus the dimensionless deflection load decreases. The stiffness enhancement is pronounced in by changing the number of layers from 1 to 5. By increasing the number of layers more than 5 layers, the enhancement of stiffness becomes insignificant.
- ✓ The FG-X CNTRC laminated nanobeams give the smallest deflections, while the highest deflections are for FG-O CNTRC beams.
- ✓ By increasing the slenderness ration of the beam, the normal stress increased dramatically relative to the increasing in shear stress.
- ✓ It is noticed that the shear stress is dependent implicitly on loading type, gradation type and slenderness ratio. However, the normal stress id dependent explicitly on loading type, gradation type and slenderness ratio
- ✓ In general, the hyperbolic shear deformation solutions in conjunction with nonlocal strain gradient theory presented here provide benchmark results, which can be used for the evaluation of different beams theories and also to compare results obtained by other approximate methods such as the finite-element method.

Acknowledgments

This research was supported by the Algerian Directorate General of Scientific Research and Technological Development (DGRSDT) and University of Mustapha Stambouli of Mascara (UMS Mascara) in Algeria.

References

Ahouel, M. Houari, M.S.A. Adda Bedia, E.A. and Tounsi, A. (2016), "Size-dependent mechanical behavior of functionally graded trigonometric shear deformable nanobeams including neutral surface position concept", *Steel Compos. Struct.*, **20**(5), 963-981. https://doi.org/10.12989/scs.2016.20.5.963.

Ait Atmane, H. Tounsi, A. and Bernard, F. (2017), "Effect of thickness stretching and porosity on mechanical response of a functionally graded beams resting on elastic foundations", *Int. J. Mech. Mater. Des*., **13**, 71-84. https://doi.org/10.1007/s10999-015-9318-x.

Akbaş, S.D. (2017), "Nonlinear static analysis of functionally graded porous beams under thermal effect", *Coupled Syst. Mech.*, **6**(4), 399-415. https://doi.org/10.12989/csm.2017.6.4.399.

Almitani, K.H., Abdelrahman, A.A. and Eltaher, M.A. (2020), "Stability of perforated nanobeams incorporating surface energy effects", *Steel Compos. Struct.*, **35**(4), 555-566. https://doi.org/10.12989/scs.2020.35.4.555.

Anirudh, B., Ben Zineb, T., Polit, O., Ganapathi, M. and Prateek, G. (2020), "Nonlinear bending of porous curved beams reinforced by functionally graded nanocomposite graphene platelets applying an efficient shear flexible finite element approach", *Int. J. Nonlinear Mech.*, **119**, 103346. https://doi.org/10.1016/j.ijnonlinmec.2019.103346.

Avhad, P.V. and Sayyad, A.S. (2020), "Static analysis of functionally graded composite beams curved in elevation using higher order shear and normal deformation theory", *Mater. Today: Proceedings*, **21**, 1195-1199. https://doi.org/10.1016/j.matpr.2020.01.069.

Aydogdu, M. and Taskin, V. (2007), "Free vibration analysis of functionally graded beams with simply supported edges", *Mater. Design*, **28**, 1651-1656. https://doi.org/10.1016/j.matdes.2006.02.007.

Barati, M.R. (2017), "Dynamic response of porous functionally graded material nanobeams subjected to moving nanoparticle based on nonlocal strain gradient theory", *Mat. Res. Express*, **4**(11), 115017. https://doi.org/10.1088/2053-1591/aa9765.

Barati, M.R. Faleh, N.M. and. Zenkour, A.M. (2018), "Dynamic response of nanobeams subjected to moving nanoparticles and hygro-thermal environments based on nonlocal strain gradient theory", *Mech. Adv. Mater. Struct.*, **26**(19), 1661-1669. https://doi.org/10.1080/15376494.2018.1444234.

Benatta, M.A., Mechab, I., Tounsi, A. and Adda Bedia, E.A. (2008), "Static analysis of functionally graded short beams including warping and shear deformation effects", *Comput. Mater. Sci.*, **44**, 765-773. https://doi.org/10.1016/j.commatsci.2008.05.020.

Bensaid, I., Daikh, A.A. and Drai, A. (2020), "Size-dependent free vibration and buckling analysis of sigmoid and power law functionally graded sandwich nanobeams with microstructural defects", *Proceedings of the institution of mechanical engineers, Part C: Journal of mechanical engineering science*. https://doi.org/10.1177/0954406220916481.

Borjalilou, V., Taati, E. and Ahmadian, M.T. (2019), "Bending, buckling and free vibration of nonlocal FG-carbon nanotube-reinforced composite nanobeams: exact solutions", *SN Applied Sciences*, **1**, 1323. https://doi.org/10.1007/s42452-019-1359-6.

Bouafia, K., Kaci, A., Houari, M.S.A., Benzair, A. and Tounsi, A. (2017), "A nonlocal quasi-3D theory for bending and free flexural vibration behaviors of functionally graded nanobeams", *Smart Struct. Syst.*, **19**(2), 115-126. https://doi.org/10.12989/sss.2017.19.2.115.

Bourada, M., Kaci, A., Houari, M.S.A. and Tounsi, A. (2015), "A new simple shear and normal deformations theory for functionally graded beams", *Steel Compos. Struct.*, **18**(2), 409-423. https://doi.org/10.12989/scs.2015.18.2.409.

Bouremana, M., Houari, M.S.A., Tounsi, A., Kaci, A. and Bedia, E.A.A. (2013), "A new first shear deformation beam theory based on neutral surface position for functionally graded beams. *Steel Compos. Struct.*, **15**(5), 467–479. https://doi.org/10.12989/scs.2013.15.5.467.

Chaht, F.L., Kaci, A., Houari, M.S.A., Tounsi, A., Beg, O.A. and Mahmoud, S.R. (2015), "Bending and buckling analyses of functionally graded material (FGM) size-dependent nanoscale beams including the thickness stretching effect", *Steel Compos. Struct.*, **18**(2), 425-442. https://doi.org/10.12989/scs.2015.18.2.425.

Chen, D., Yang, J. and Kitipornchai, S, (2015), "Elastic buckling and static bending of shear deformable functionally graded porous beam", *Compos. Struct.*, **133**, 54-61. http://dx.doi.org/10.1016/j.compstruct.2015.07.052.

Daikh, A.A., Bachiri, A., Houari, M.S.A. and Tounsi, A. (2020), "Size dependent free vibration and buckling of multilayered carbon nanotubes reinforced composite nanoplates in thermal environment", *Mech. Based Design Struct. Mach.*, https://doi.org/10.1080/15397734.2020.1752232.

Daikh, A.A., Bensaid, I., Bachiri, A., Houari, M.S.A., Tounsi, A. and Merzouki, T. (2020), "On static bending of multilayered carbon nanotube-reinforced composite plates", *Comput. Concrete*, **26**(2), 137-150. https://doi.org/10.12989/cac.2020.26.2.000

Daikh, A.A., Guerroudj, M., Elajrami, M. and Megueni, A. (2020), "Thermal Buckling of Functionally Graded Sandwich Beams, *Adv. Mater. Res*., **1156**, 43-59. https://doi.org/10.4028/www.scientific.net/AMR.1156.43.

Daikh, A.A., Houari, M.S.A. and Tounsi, A. (2019), "Buckling analysis of porous FGM sandwich nanoplates due to heat conduction via nonlocal strain gradient theory", *Eng. Res. Express*, **1**, 015022. https://doi.org/10.1088/2631-8695/ab38f9.

Ding, J.H., Huang, D.J. and Chen, W.Q. (2007), "Elasticity solutions for plane anisotropic functionally graded beams", *Int. J. Solids Struct*., **44**(1), 176-196. https://doi.org/10.1016/j.ijsolstr.2006.04.026.

Ebrahimi, F. and Barati, M.R. (2016a), "Through-the-length temperature distribution effects on thermal vibration analysis of nonlocal strain-gradient axially graded nanobeams subjected to nonuniform magnetic field", *J. Therm. Stresses*, **40**(5), 548-563. https://doi.org/10.1080/01495739.2016.1254076.

Ebrahimi, F. and Barati, M.R. (2016b), "Size-dependent dynamic modeling of inhomogeneous curved nanobeams embedded in elastic medium based on nonlocal strain gradient theory", *Proceedings of the institution of mechanical engineers, Part C: Journal of mechanical engineering science*, **231**(23), 4457-4469. https://doi.org/10.1177/0954406216668912.

Ebrahimi, F. and Barati, M.R. (2016c), "Nonlocal strain gradient theory for damping vibration analysis of viscoelastic inhomogeneous nano-scale beams embedded in visco-Pasternak foundation", *J. Vib. Control*, **24**(10), 2080-2095. https://doi.org/10.1177/1077546316678511.

Ebrahimi, F. and Barati, M.R. (2017a), "A nonlocal strain gradient refined beam model for buckling analysis of size-dependent shear-deformable curved FG nanobeams", *Compos. Struct.*,

159, 174-182. https://doi.org/10.1016/j.compstruct.2016.09.058.

Ebrahimi, F. and Barati, M.R. (2017b), "Flexural wave propagation analysis of embedded S-FGM nanobeams under longitudinal magnetic field based on nonlocal strain gradient theory", *Arabian J. Sci. Eng.*, **42**(5), 1715-1726. https://doi.org/10.1007/s13369-016-2266-4.

Ebrahimi, F. and Barati, M.R. (2017c), "Longitudinal varying elastic foundation effects on vibration behavior of axially graded nanobeams via nonlocal strain gradient elasticity theory", *Mech. Adv. Mater. Struct.*, **25**(11), 953-963. https://doi.org/10.1080/15376494.2017.1329467.

Ebrahimi, F. and Barati, M.R. (2018), "Damping vibration behavior of visco-elastically coupled double-layered graphene sheets based on nonlocal strain gradient theory", *Smart Mater. Struct.*, **26**(6), 065018. https://doi.org/10.1007/s00542-017-3529-z.

Eltaher, M.A. Emam, S.A. Mahmoud, F.F. (2013), "Static and stability analysis of nonlocal functionally graded nanobeams", *Compos. Struct.*, **96**, 82-88. https://doi.org/10.1016/j.compstruct.2012.09.030.

Eltaher, A.M., Fouda, N., El-midany, T. and Sadoun, A.M. (2018), "Modified porosity model in analysis of functionally graded porous nanobeams", *J. Braz. Soc. Mech. Sci. Eng.*, **40**, 141. https://doi.org/10.1007/s40430-018-1065-0.

Eltaher, M.A. and Abdelrahman, A.A. (2020), "Bending behavior of squared cutout nanobeams incorporating surface stress effects", *Steel Compos. Struct.*, **36**(2), 143-161. http://dx.doi.org/10.12989/scs.2020.36.2.143.

Eringen, A.C. (1983), "On differential equations of nonlocal elasticity and solutions of screw dislocation and surface waves", *J. Appl. Phys.*, **54**, 4703-4710. https://doi.org/10.1063/1.332803.

Fahsi, B.. Bachir Bouiadjra, B., Mahmoudi, A., Benyoucef, S. and Tounsi, A. (2013), "Assessing the effects of porosity on the bending, buckling, and vibrations of functionally graded beams resting on an elastic foundation by using a new refined quasi-3d theory", *Mech. Compos. Mater.*, **55**(2), 219-230. https://doi.org/10.1007/s11029-019-09805-0.

Feng, C., Kitipornchai, S. and Yang, J. (2017), "Nonlinear free vibration of functionally graded polymer composite beams reinforced with graphene nanoplatelets (GPLs)", *Eng. Struct.*, **140**, 110-119. http://dx.doi.org/10.1016/j.engstruct.2017.02.052.

Fouda, N., El-midany, T. and Sadoun, A.M. (2017), "Bending, Buckling and Vibration of a Functionally Graded Porous Beam Using Finite Elements", *J. Appl. Comput. Mech.*, **3**(4), 274-282. https://doi.org/10.22055/JACM.2017.21924.1121

Ghorbanpour Arani, A. and Zamani, M.H. (2018), "Bending analysis of agglomerated carbon nanotube-reinforced beam resting on two parameters modified Vlasov model foundation", *Indian J. Phys.*, **92**, 767-777. https://doi.org/10.1007/s12648-018-1162-z.

Hadji, L., Daouadji, T.H., Meziane, M., Ait Amar. Tlidji, Y. and Adda Bedia, E.A. (2016), "Analysis of functionally graded beam using a new first-order shear deformation theory", *Struct. Eng. Mech.*, **57**(2), 315-325. https://doi.org/10.12989/sem.2016.57.2.315.

Hadji, L., Hassaine Daouadji, T., Tounsi, A. and Bedia, E.A. (2015a), "A n-order refined theory for bending and free vibration of functionally graded beams", *Struct. Eng. Mech.*, **54(**5), 923-936. https://doi.org/10.12989/sem.2015.54.5.923

Hadji, L., Khelifa, Z. and Adda Bedia, E.A. (2016), "A New Higher Order Shear Deformation Model for Functionally Graded Beams", *KSCE J. Civ. Eng.*, **20**, 1835-1841. https://doi.org/10.1007/s12205-015-0252-0.

Hadji, L., Khelifa, Z., Daouadji, T.H. and Bedia, E.A. (2015b), "Static bending and free vibration of FGM beam using an exponential shear deformation theory", *Coupled Syst. Mech.*, **4**(1), 99-114. https://doi.org/10.12989/CSM.2015.4.1.099.

Hadji, L., Zouatnia, N. and Bernard, F. (2018), "An analytical solution for bending and free vibration responses of functionally graded beams with porosities: Effect of the micromechanical models", *Struct. Eng. Mech.*, **69**(2), 231-241. https://doi.org/10.12989/sem.2019.69.2.231.

Hamed, M.A., Abo-bakr, R.M., Mohamed, S.A. and Eltaher, M.A. (2020), "Influence of axial load function and optimization on static stability of sandwich functionally graded beams with porous core", *Eng. with Comput.*, 1-18. https://doi.org/10.1007/s00366-020-01023-w.

Hassaine Daouadji, T., Henni, A.H., Tounsi, A. and Bedia, E.A.A. (2013), "Elasticity solution of a cantilever functionally graded beam", *Appl. Compos. Mater.*, **20**(1), 1-15. https://doi.org/10.1007/s10443-011-9243-6.

Heshmati, M. and Daneshmand, F. (2018), "Vibration analysis of non-uniform porous beams with functionally graded porosity distribution", *J Mater.: Design Appl.*, **233**(8), 1678-1697. https://doi.org/10.1177/1464420718780902.

Kadoli, R., Akhtar, K. and Ganesan, N. (2008), "Static analysis of functionally graded beams using higher order shear deformation theory", *Appl. Math. Model.*, **32**, 2509-2525. https://doi.org/10.1016/j.apm.2007.09.015.

Lim, C.W., Zhang, G. and Redd, J.N. (2015), "A higher-order nonlocal elasticity and strain gradient theory and its applications in wave propagation", *J. Mech. Phys. Solids*, **78**, 298-313. https://doi.org/10.1016/j.jmps.2015.02.001.

Lu, C.F., Chen, W.Q., Xu, R.Q. and Lim, C.W. (2008), "Semi-analytical elasticity solutions for bi-directional functionally graded beams", *Int. J. Solids Struct.*, **45**, 258-275. https://doi.org/10.1016/j.ijsolstr.2007.07.018.

Malikan, M. and Eremeyev, V.A. (2020), "A new hyperbolic-polynomial higher-order elasticity theory for mechanics of thick FGM beams with imperfection in the material composition", *Compos. Struct.*, **249**, 112486. https://doi.org/10.1016/j.compstruct.2020.112486.

Mayandi, K. and Jeyaraj, P (2003), "Bending, buckling and free vibration characteristics of FG-CNT-reinforced polymer composite beam under non-uniform thermal load", *J Mater. Design Appl.*, **229**, 13-28. http://dx.doi.org/10.1177/1464420713493720.

Meradjah, M., Kaci, A., Houari, M.S.A., Tounsi, A. and Mahmoud, S.R. (2015), "A new higher order shear and normal deformation theory for functionally graded beams", *Steel Compos. Struct.*, **18**(3), 793-809. https://doi.org/10.12989/scs.2015.18.3.793

Mirjavadi, S.S., Afshari, B.M., Barati, M.R. and Hamouda, A.M.S. (2020), "Transient response of porous inhomogeneous nanobeams due to various impulsive loads based on nonlocal strain gradient elasticity", *Int. J. Mech. Mater. Design*, **16**(1), 57-68. https://doi.org/10.1007/s10999-019-09452-2.

Ould Larbi, L., Kaci, A., Houari, M.S.A. and Tounsi, A. (2013), "An efficient shear deformation beam theory based on neutral surface position for bending and free vibration of functionally graded beams", *Mech. Based Design Struct. Mach.*, **41**(4), 421-433, https://doi.org/10.1080/15397734.2013.763713.

Pradhan, S.C. and Mandal, U. (2013), "Finite element analysis of CNTs based on nonlocal elasticity and Timoshenko beam theory including thermal effect", *Physica E*, **53**, 223-232. http://dx.doi.org/10.1016/j.physe.2013.04.029.

Sahmani, S., Mohammadi Aghdam, M. and Rabczuk, T. (2018), "Nonlinear bending of functionally graded porous micro/nano-beams reinforced with graphene platelets based upon nonlocal strain gradient theory", *Compos. Struct.*, **186**, 68-78. https://doi.org/10.1016/j.compstruct.2017.11.082.

Salari, E., Sadough Vanini, S.A., Ashoori, R.A. and Akbarzadeh, H.A. (2020), "Nonlinear thermal behavior of shear deformable FG porous nanobeams with geometrical imperfection: Snapthrough and postbuckling analysis", *Int. J. Mech. Sci.*, **178**, 105615. https://doi.org/10.1016/j.ijmecsci.2020.105615.

Sallai, B., Hadji, L., Daouadji, T.H. and Adda Bedia, E.A. (2015), "Analytical solution for bending analysis of functionally graded beam", *Steel Compos. Struct.*, **19**(4), 829-841. https://doi.org/10.12989/SCS.2015.19.4.829.

Salvetat, D. and Rubio, A. (2002), "Mechanical properties of carbon nanotubes: a fiber digest for beginners", *Carbon*, **40**,1729-1734. https://doi.org/10.1016/S0008-6223(02)00012-X.

Sankar, B.V. (2001), "An elasticity solution for functionally graded beams", *Compos. Sci. Technol.*, **61**(5), 689-696. https://doi.org/10.1016/S0266-3538(01)00007-0.

Sayyad, S.A. and Ghugal, Y.M. (2018), "An inverse hyperbolic theory for FG beams resting on Winkler-Pasternak elastic foundation", *Adv. Aircraft Spacecraft Sci.*, **5**(6), 671-689. https://doi.org/10.12989/aas.2018.5.6.671.

Shen, H.C., Lin, F. and Xiang, Y. (2017), "Nonlinear bending and thermal postbuckling of functionally graded graphene-reinforced composite laminated beams resting on elastic foundations", *Eng. Struct.*, **140**, 89-97. http://dx.doi.org/10.1016/j.engstruct.2017.02.069.

Sobhy, M. (2020), "Differential quadrature method for magneto-hygrothermal bending of functionally graded graphene/Al sandwich-curved beams with honeycomb core via a new higher-order theory", *J. Sandw. Struct. Mater.*, https://doi.org/10.1177/1099636219900668.

Tran, T.T., Pham, Q.H. and Nguyen-Thoi, T. (2020), "Static and free vibration analyses of functionally graded porous variable-thickness plates using an edge-based smoothed finite element method", *Defence Technol.*, https://doi.org/10.1016/j.dt.2020.06.001.

Wang, Y., Xie, K., Fu, T. and Shi, C. (2019), "Bending and elastic vibration of a novel functionally graded polymer nanocomposite beam reinforced by graphene nanoplatelets", *Nanomaterials*, **9**, 1690. https://doi.org/10.3390/nano9121690.

Wattanasakulpong, N. and Ungbhakorn, V. (2013), "Analytical solutions for bending, buckling and vibration responses of carbon nanotube-reinforced composite beams resting on elastic foundation", *Comput. Mater. Sci.*, **71**, 201-208. http://dx.doi.org/10.1016/j.commatsci.2013.01.028.

Yas, M.H. and Samadi, N. (2012), "Free vibrations and buckling analysis of carbon nanotube-reinforced composite Timoshenko beams on elastic foundation", *Int. J. Press. Vessels Pip.*, **98**, 119-128. http://dx.doi.org/10.1016/j.ijpvp.2012.07.012.

Ying, J., Lu, C.F. and Chen, W.Q. (2008), "Two-dimensional elasticity solutions for functionally graded beams resting on elastic foundations", *Compos. Struct.*, **84**(3), 209-219. https://doi.org/10.1016/j.compstruct.2007.07.004.

Zghal, S., Ataoui, D. and Dammak, F. (2020), "Static bending analysis of beams made of functionally graded porous materials", *Mech. Based Design Struct. Mach.*, https://doi.org/10.1080/15397734.2020.1748053.

Zhao, X., Zheng, S. and Li, Z. (2020), "Effects of porosity and flexoelectricity on static bending and free vibration of AFG piezoelectric nanobeams", *Thin-Wall. Struct.*, **151**, 106754. https://doi.org/10.1016/j.tws.2020.106754.

Zhong, Z. and Yu, T. (2007), "Analytical solution of a cantilever functionally graded beam", *Compos. Sci. Technol.*, **67**(3-4), 481-488. https://doi.org/10.1016/S0266-3538(01)00007-0.

Zidi, M., Houari, M.S.A., Tounsi, A., Bessaim, A. and Mahmoud, S.R. (2017), "A novel simple two-unknown hyperbolic shear deformation theory for functionally graded beams", *Struct. Eng. Mech.*, **64**(2), 145-153. https://doi.org/10.12989/sem.2017.64.2.145.

Zouatnia, N. Hadji, L. and Kassoul, A. (2017), "A refined hyperbolic shear deformation theory for bending of functionally graded beams based on neutral surface position", *Struct. Eng. Mech.*, **63**(5), 683-689. https://doi.org/10.12989/sem.2017.63.5.683.

Zouatnia, N., Hadji, L. and Kassoul, A. (2019), "An analytical solution for bending and vibration responses of functionally graded beams with porosities", *Wind Struct.*, **25**(4), 329-342. https://doi.org/10.12989/was.2017.25.4.329.

CC